Journal of Civil Engineering and Architecture 12 (2018) 651-661
doi: 10.17265/1934-7359/2018.09.005

Modeling of Bridging Law for PVA Fiber-Reinforced Cementitious Composite Considering Fiber Orientation

Yuriko Ozu[1], Masaru Miyaguchi[1] and Toshiyuki Kanakubo[2]

1. Sumitomo Mitsui Construction Co., Ltd., Chuo-ku, Tokyo 104-0051, Japan

2. Department of Engineering Mechanics and Energy, University of Tsukuba, Tsukuba-city, Ibaraki 305-8573, Japan

Abstract: The authors have proposed the calculation method of bridging law, that is expressed by tensile stress–crack width relationship, considering the influence of fiber orientation in FRCC (fiber-reinforced cementitious composite). The objective of this study is to propose a new tri-linear model that expresses the bridging law considering fiber orientation. The parameters that give the characteristic points of the tri-linear model are proposed as functions of orientation intensity. The bending test, in which the specimens are fabricated by three different casting methods, is conducted to verify the adaptability of the proposed model. The results of section analysis using the proposed model can present the difference of bending strength due to the fiber orientation.

Key words: FRCC, tensile stress, crack width, tri-linear model, fiber orientation, PVA fiber, bending test, compacting vibrator.

1. Introduction

FRCC (fiber-reinforced cementitious composite), in which short discrete fibers of a certain percentage in volume fraction are mixed in mortar or concrete, is cementitious material that shows higher tensile and bending performance comparing with conventional concrete. The elements such as coupling beams and seismic walls using SHCC (strain hardening cement composites), that show tensile strain hardening and multiple fine cracks, provide very ductile behavior with small crack opening (e.g. [1]). These characterized performances of FRCC are brought by bridging effect of fibers at cracks in the matrix. However, some previous studies have reported that the tensile characteristics even in SHCC are influenced by fiber orientation in matrix (e.g. [2]). Casting and pouring direction of FRCC affects the fiber orientation, and vertical pouring in tension test specimens causes degradation of tensile strength and deformation capacity of FRCC.

Corresponding author: Toshiyuki Kanakubo, professor, research fields: concrete structures, cementitious composites, FRP for concrete strengthening and seismic performance of concrete structures.

The authors have studied the influence of fiber orientation to tensile characteristics of FRCC using PVA (polyvinyl alcohol) fiber through visualization simulation using water glass solution and calculation of the bridging law, which is expressed by tensile stress–crack width relationship [3]. To evaluate the fiber orientation distribution quantitatively, an approximation methodology using an elliptic function (elliptic distribution) was introduced in that study. The bridging law is calculated considering the elliptic distribution, the snubbing effect [4], and the fiber strength degradation [5]. The calculated bridging laws can show good agreements with the results of the tension test in which the specimens were fabricated by horizontal and vertical casting. However, it is difficult to use calculated bridging laws directly for evaluation of characteristics of FRCC elements such as beams and columns, because the shape of bridging laws which are expressed by tensile stress and crack width is strongly affected by fiber orientation. It is considered that simpler models for bridging laws make evaluations of FRCC elements easier.

Many types of tensile stress–crack width models for bridging laws can be considered. For example,

multi-function models, multi-linear models, tri-linear models, and bi-linear models have been introduced for tensile stress–strain models of FRCC [2]. In this study, a tri-linear model shown in Fig. 1 is chosen to describe the characteristic points in calculated bridging laws considering the phenomena those occur in single fiber pullout properties. The modeled bridging laws are used for section analysis of bending test specimens to verify their adaptability. The modeled bridging laws are characterized by fiber orientation, so the bending specimens are fabricated by three casting methods to vary the fiber orientation.

At first, calculation method of bridging laws proposed by authors is briefly introduced in next chapter.

2. Calculation Method of Bridging Law

The authors have proposed the bridging law, which is expressed by tensile stress–crack width relationship, considering the influence of fiber orientation [3]. The bridging law is calculated by the summation of the pullout properties of each single fiber in crack surface. The model of the pullout load–pullout displacement relationship of the single fiber is shown in Fig. 2. The pullout load–pullout displacement relationship is modeled by tri-linear model considering chemical and frictional bond between PVA fiber and matrix [5]. At the time of the first peak load P_a, the chemical bond is debonded over the entire length of fiber. After that, the pullout load increases to maximum load P_{max} because of the frictional bond. The pullout load becomes zero when the crack width corresponds to the embedded length of the single fiber, l_b. The crack width at the first peak load, w_a, is twice the value of the pullout displacement, δ_{pull}. The crack width at the maximum load, w_{max}, is 1.5 times the pullout displacement because the pullout displacement on the end of long embedded length starts decreasing when the pullout load begins to decrease on the end of short embedded length.

The pullout property of single fiber varies due to snubbing effect and fiber strength degradation by orientation angle, ψ. Snubbing effect shows the increment of pullout load due to the reaction force at the embedding edge of fiber when fiber has orientation angle [4]. Fiber strength degradation shows the decreasing of fiber strength in the case of polymer fiber due to the surface of fiber roughed by the embedding edge when fiber is embedded obliquely with normal direction of crack surface [5]. As shown in Fig. 2, though the pullout load increases with increasing of orientation angle by the snubbing effect, fiber tends to rupture by the fiber strength degradation if orientation angle becomes large.

In order to give the orientation angle to each single fiber at crack surface in the calculation of the bridging law, a PDF (probability density function) has been proposed by Kanakubo et al. [3]. The PDF expresses the fiber orientation distribution using elliptic distribution. The fiber orientation varies by the value of orientation intensity k (ratio of the two radii of elliptic function) and principal angle θr (argument of

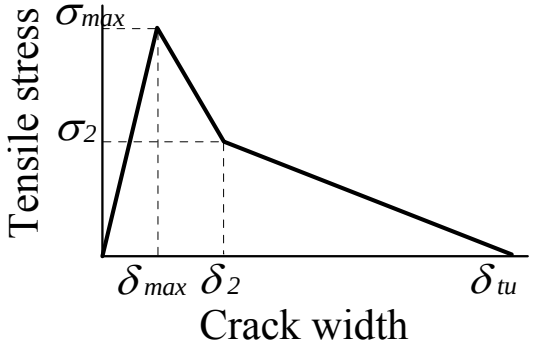

Fig. 1 Proposed tri-linear model for bridging law.

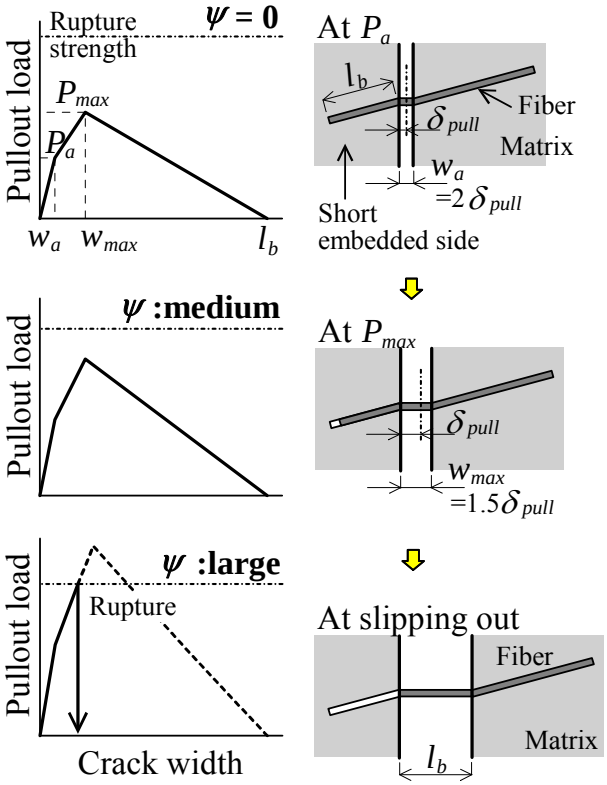

Fig. 2 Pullout model of a single fiber.

one radius of elliptic function). The random orientation is given by $k = 1$. When the value of k is larger than 1, fibers tend to orient toward θr. When the value of k is smaller than 1, fibers tend to orient toward the perpendicular to θr.

Tensile stress is calculated by the summation of the pullout load of each single fiber at crack surface as given in Eqs. (1) and (2).

$$\sigma_{bridge} = \frac{P_{bridge}}{A_m} = \frac{V_f}{A_f} \cdot \sum_h \sum_j \sum_i P_{ij}(w,\psi) \cdot p_{xy}(\theta_i) \cdot p_{zx}(\phi_j) \cdot p_x(y_h, z_h) \cdot \Delta\theta \cdot \Delta\phi \cdot (\Delta y \cdot \Delta z) \quad (1)$$

$$P = P_{pull} \cdot e^{f \cdot \psi} < P_{rup} \cdot e^{-f' \cdot \psi} \quad (2)$$

where,

σ_{bridge} = tensile stress;

P_{bridge} = bridging force (= total of pullout load);

A_m = cross-sectional area of matrix;

V_f = fiber volume fraction;

A_f = cross-sectional area of a single fiber;

P = pullout load of a single fiber;

P_{pull} = pullout load of a single fiber at a zero fiber angle;

P_{rup} = pullout load of a single fiber at rupture at a zero fiber angle;

F = snubbing coefficient;

f' = fiber strength reduction factor;

p_{xy}, p_{zx} = probability by elliptic distribution;

p_x = probability of fiber distribution along x-axis;

ψ = fiber angle to x-axis;

θ = angle between x-axis and projected line of the fiber to x-y plane;

ϕ = angle between x-axis and projected line of the fiber to z-x plane.

The PDF, p_x (y, z), gives the probability for the existence of the fiber in the x-axis direction. In this study, p_x (y, z) is assumed to be constant. This means that the fibers are randomly distributed along the longitudinal direction of the specimen.

The calculated bridging laws for the orientation

intensity k from 0.1 to 10 are shown in Fig. 3. The parameters for the calculation are listed in Table 1. The principal angle θr is set to 0° (axial direction of the specimen). The curves in Fig. 3 do not include the crack strength to exhibit the stress due to only bridging force of fibers. As shown in Fig. 3, tensile stress significantly drops after the maximum stress, then moderate decrement follows. The significant drop and moderate decrement of the tensile stress in the calculation after the maximum stress is caused by rupture and pullout of fibers, respectively. The maximum tensile stress in the bridging law remarkably increases with the increment of the value of k, i.e., stronger fiber orientation to the normal direction of crack surface.

3. Modeling of Bridging Law

As described in the former chapter, the calculated bridging laws are strongly affected by fiber orientation. Proposing simpler models for bridging laws can make evaluations of FRCC elements easier. In this study, a tri-linear model shown in Fig. 1 is newly proposed to express tensile stress–crack width relationship of FRCC after first cracking considering the fiber orientation.

From Fig. 3, the bridging law is characterized by three parts, i.e., the part from the origin to maximum tensile stress, the part of the significant drop of tensile stress after maximum tensile stress, and the part of moderate decrement of tensile stress. Therefore, the tri-linear model of the bridging law is considered to be suitable as shown in Fig. 1. The model has five parameters: the maximum tensile stress, σ_{max}, the crack width at σ_{max}, δ_{max}, the second point tensile stress after the significant drop of stress, σ_2, the crack width at σ_2, δ_2, and the crack width at the loss of stress, δ_{tu}. δ_{tu} is constant value, because fiber is completely pulled out when crack width becomes half of fiber length.

Remaining four parameters in the model are expressed as a function of the orientation intensity k to simplify the modeling of the bridging law. The

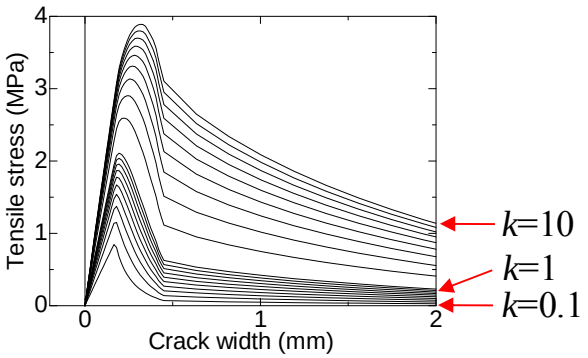

Fig. 3 Calculation result of bridging law.

Table 1 Parameters for calculation of bridging law.

Parameter	Input value
Fiber volume fraction, V_f	2.0%
Fiber length, l_f	12 mm
Fiber diameter, d_f	0.10 mm
First peak load, P_a	1.5 N
Crack width at P_a, w_a	0.20 mm
Maximum load, P_{max}	3.0 N
Crack width at P_{max}, w_{max}	0.45 mm
Fiber effective strength	569 MPa
Snubbing coefficient, f	0.5
Fiber strength reduction factor, f'	0.3

relationship between the parameters for stress and k are shown in Fig. 4. The relationship between the parameters for crack width and k are shown in Fig. 5. The dotted lines in all figures exhibit the regression calculation results for the values of the parameters by the least squares method. The solid lines exhibit the modified regression calculation result to simplify the relational expression between each parameter and k, and they are shown in each figure. The stress values in Fig. 4 are decided to be expressed by the function which starts from the origin because the bridging force becomes zero in the case of $k \rightarrow 0$, i.e., no bridging fiber exists. The function for δ_{max} is decided to pass the point of calculated value of δ_{max} at $k = 1$ (random orientation). From the calculation results of bridging law, δ_2 corresponds with the crack width at the maximum pullout load of single fiber in Table 1, i.e., constant value of 0.45 mm.

4. Bending Test of FRCC Varying Fiber Orientation

The bending test of PVA-FRCC is conducted to verify the adaptability of the modeled bridging law through section analysis. The bending test specimens are fabricated by three casting methods to vary the fiber orientation.

4.1 Specimens and Used Materials

The dimension of the specimens applied in this study is shown in Fig. 6. Specimens are the notched beams which have the cross-section of 100 mm × 100 mm and a notch with a depth of 30 mm and a width of 5 mm by a concrete cutter after FRCC become hardened. The position of a notch and a casting direction is as shown in Fig. 6. These dimensions and manufacturing procedures follow ISO 19044 [6]. The experimental parameter is the placing method of FRCC using the compacting vibrator explained after. Six specimens were manufactured for each parameter, and total of 18 specimens were tested.

PVA fiber of 0.10 mm diameter and 12 mm length were utilized in this study. The mix proportion of PVA-FRCC is shown in Table 2. The volume fraction of PVA fiber is 2.0%. FRCC in this study has self-compacting behavior. The average of compressive strength in the material age at bending tests was 34.6 MPa

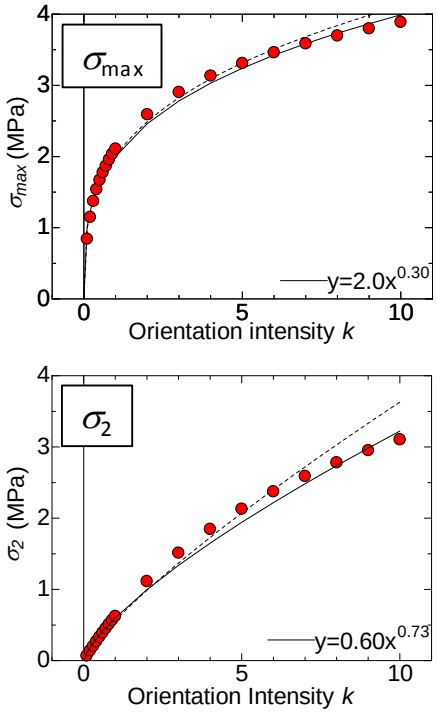

Fig. 4 Stress parameters for tri-linear model.

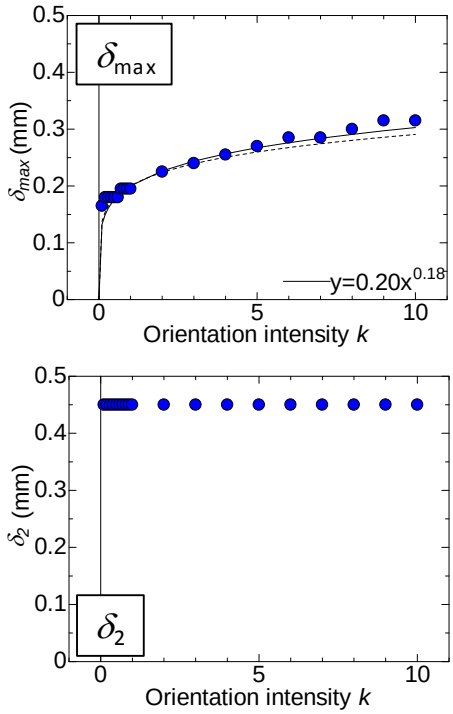

Fig. 5 Crack width parameters for tri-linear model.

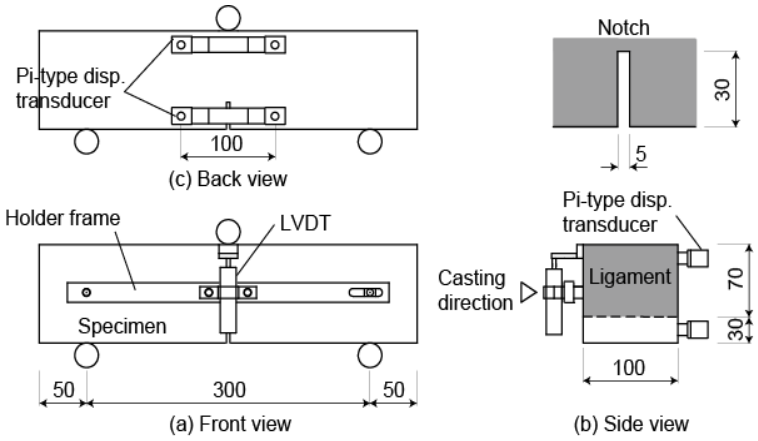

Fig. 6 Notched beam specimen for bending test (unit: mm).

Table 2 Mix proportion of PVA-FRCC.

Fiber volume fraction	Water by binder ratio	Sand by binder ratio	Unit weight (kg/m^3)			
			Water	Cement	Fly ash	Sand
2.0%	0.39	0.50	380	678	291	484

Cement: High early strength Portland cement, Fly ash: Type II of JIS A 6202.
Sand: Size under 0.2 mm, Super plasticizer: Binder × 0.6%.

by ϕ100 mm × 200 mm cylinder test pieces.

4.2 Placing of FRCC

Many researches have studied the effects of fiber orientation on the mechanical characteristics of FRCC, including FRC (fiber-reinforced concrete). The scheme of the current approach to evaluate the fiber orientation has considered the casting method, fresh-state properties, flow, vibration, and formwork geometry (e.g. [7]). The authors have studied the

effect of a compacting vibrator to bending characteristics of FRCC beams [8]. The bending capacity and ductility increases by applying a compacting vibrator after pouring FRCC. It is suggested that the fiber orientation tends to differ in each specimen by observing the specimen sections after loading. So, the method of applying a compacting vibrator is also introduced in this study to vary the fiber orientation of specimens.

Fig. 7 shows the three series of compacting methods of FRCC: (a) SC (self-compacting) without vibrating; (b) VF (vibrator-fix); and (c) VM (vibrator-move). A vibrator with a 24.5 mm diameter rod, and vibrating frequency of 200 Hz, which is commonly used for compacting of conventional concrete, was used.

SC is standard placing method in which FRCC is continuously poured from the edge of the mold with the slope of 1/33. In VF compacting, the vibrator is set with vibration at the center of the specimen after FRCC is poured into the mold. The vibration period is 10 s. VM compacting is the method in which the vibrator is moved and reciprocated with vibration from the end of the mold to the other end after FRCC pouring. The vibration period is also 10 s.

The examples of photos of the specimens of VF and VM are shown in Fig. 8. As shown in Fig. 8, in the case of VF, FRCC matrix showed a circular motion with a central focus on the vibrating rod, i.e., fibers tend to orient concentrically. In the case of VM, FRCC matrix flowed longitudinally following movement of the vibrating rod. These observations indicate that fibers in FRCC tend to orient toward the axial direction along the flow.

4.3 Method of Loading and Measurements

Fig. 9 shows the bending test setup. Three-point bending tests were conducted based on ISO 19044 [6] using the displacement controlled universal loading machine of 2,000 kN capacity. The speed of the cross-head was set to 0.5 mm/min. Measurement items were load, axial deformation in central part of the specimen (gauge length = 100 mm) using two pi-type displacement transducers, and the LPD (loading

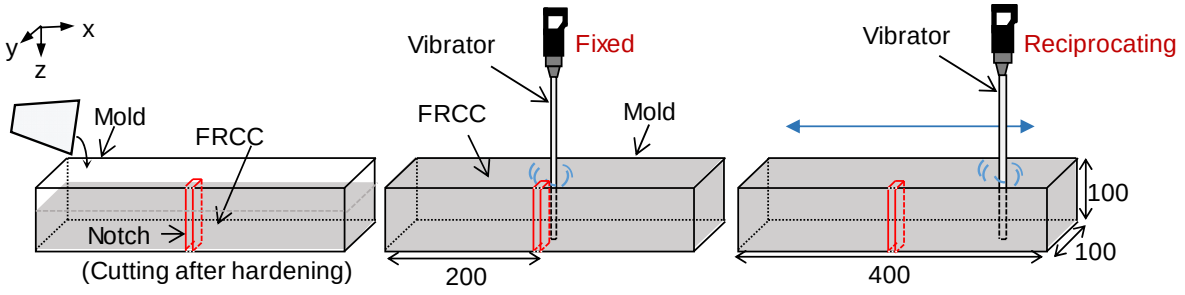

(a) SC (self compacting) **(b) VF (vibrator-fix)** **(c) VM (vibrator-move)**

Fig. 7 Compacting method (unit: mm).

(a) VF (vibrator-fix) **(b) VM (vibrator-move)**

Fig. 8 Manufacturing and vibrating of specimen.

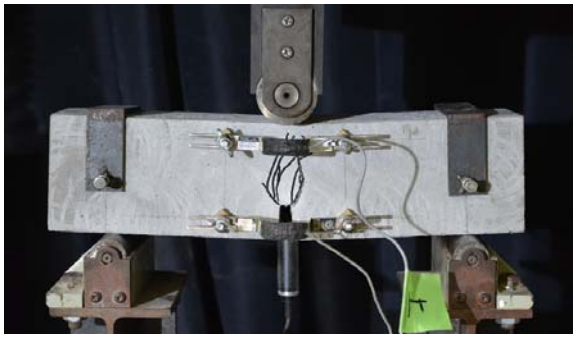

Fig. 9 Bending test setup.

point displacement) using a LVDT as shown in Fig. 6.

4.4 Test Results

The examples of the specimens of each placing method after loading are shown in Fig. 10. All specimens had plural cracks and fractured with localizing the opening of one crack after maximum load. In the case of SC specimens (self-compacting), rectilinear cracks took place perpendicularly to axial direction of the specimen. In the VF specimens (vibrator-fix), curved cracks were observed. It is considered that the curved cracks occurred due to the fiber orientation like concentric circles centering the point of vibrating. This assumes that cracks tend to progress along the weaker parts in the matrix, in which fibers orient toward crack direction and weaker bridging effect provides. In the case of VM specimens (vibrator-move), there were more cracks than those in the specimens SC and VF. It is suggested that the tendency of fiber orientation toward the axial direction in the VM specimen causes more cracks by stronger bridging effect.

Fig. 11 shows the load–CMOD (crack mouth opening displacement) curves of all specimens. CMOD was calculated as the axial deformation at the undersurface of the specimen from the measured axial deformation by pi-type displacement transducers. The points of the maximum load are plotted by circles. As shown in Fig. 11, load gradually increased after first cracking in all specimens. After the peak load, the load slightly decreased with the repetition of increase and decrease of the load. Table 3 shows the summary of the bending test results. Fracture energy in Table 3 is calculated by the following Eq. (3).

$$G_F = \frac{W}{A_{lig}} \tag{3}$$

where,

G_F = fracture energy;

W = area below load–LPD curve up to 15 mm;

A_{lig} = area of ligament.

The maximum loads of the VM specimens are twice larger than those of the SC specimens, and the fracture energies of the VM specimens are largest of all. It is considered that the bridging effect is improved by moving a vibrator. In the case of the VF specimens, the maximum loads show larger scattering comparatively.

5. Adaptability of Modeled Bridging Laws

The modeled bridging laws are used in section analysis to verify their adaptability through the evaluation of bending strength of the specimens explained in former chapter.

5.1 Section Analysis

In order to evaluate the bending strength, the section analysis based on the modeled bridging law is conducted. Fig. 12 shows whole stress–crack width model applied for the section analysis. The tensile stress–crack width model is the tri-linear model proposed in this study expressed as the functions shown in Fig. 4 and Fig. 5. The compression side is assumed to keep elasticity. The section analysis is carried out based on the assumption that plain section

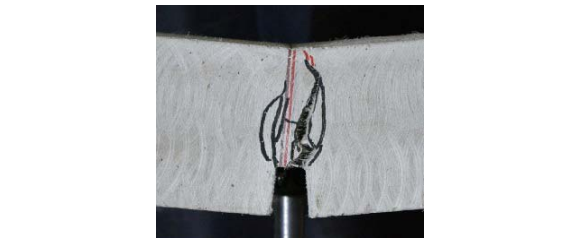

(a) SC (self compacting)

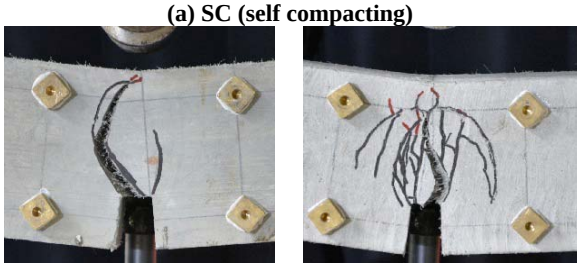

(b) VF (vibrator-fix) (c) VM (vibrator-move)

Fig. 10 Examples of specimens after loading.

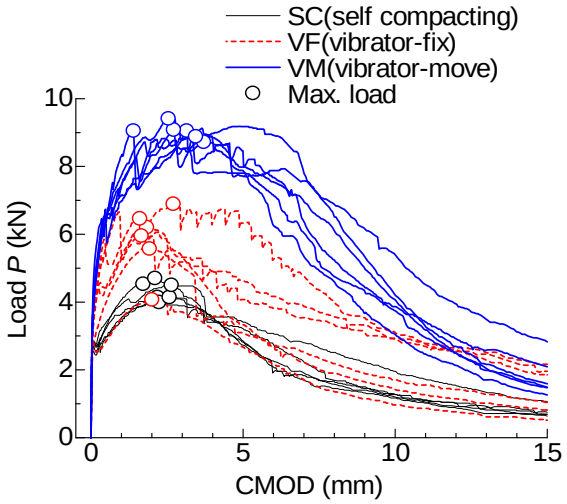

Fig. 11 Load–CMOD curves.

remains plain under considering the plain section's deformation. Firstly, arbitrary angle of rotation is given. Secondly, the crack width of each element in cross-section is calculated from linear distribution of deformation and the stress in each element of cross-section is obtained from Fig. 12. Finally, neutral axis satisfying equilibrium condition is found numerically and bending moment is calculated. The section analysis is conducted by varying orientation intensity k in the bridging law model.

The compressive stress–compressive deformation model is elastic based on the compression test results of cylinder test pieces. However, compressive strain instead of deformation is obtained from the compression test. In order to convert the strain into the deformation, equivalent compressive length $l_{c,eq}$ is introduced. The equivalent compressive length is determined to fit the initial slope between the result of section analysis and measured load–CMOD curves in the bending test. The stiffness in compressive stress–compressive deformation model is given by elastic modulus measured in compression test (E_c) divided by $l_{c,eq}$.

5.2 Comparison of Analysis and Test Results

The comparison of the maximum bending moment between the results of section analysis and bending

Table 3 Bending test results.

Placing method	ID	At maximum load		Fracture energy (N/mm)
		Max. load (kN)	CMOD (mm)	
SC	SC-1	4.53	-	4.15
	SC-2	4.14	2.19	3.58
	SC-3	3.99	2.24	3.47
	SC-4	4.14	2.58	3.17
	SC-5	4.50	2.65	3.26
	SC-6	4.70	2.11	3.51
	Average	4.33	2.35	3.52
	STDV	0.28	0.24	0.34
VF	VF-1	6.20	1.84	4.46
	VF-2	6.46	1.61	4.21
	VF-3	5.95	1.66	4.46
	VF-4	6.89	2.71	7.65
	VF-5	5.57	1.93	4.24
	VF-6	4.07	2.01	3.02
	Average	5.85	1.96	4.67
	STDV	0.98	0.40	1.55
VM	VM-1	9.05	1.40	10.2
	VM-2	9.05	3.15	9.01
	VM-3	9.08	2.72	8.20
	VM-4	8.72	3.71	8.69
	VM-5	9.41	2.55	9.74
	VM-6	8.88	3.45	7.03
	Average	9.03	2.83	8.81
	STDV	0.23	0.82	1.13

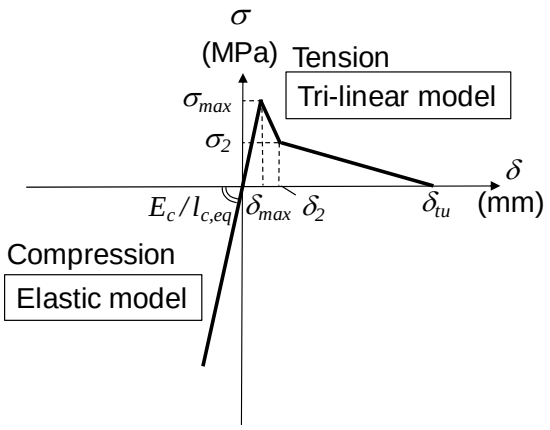

Fig. 12 Stress–crack width (deformation) model for section analysis.

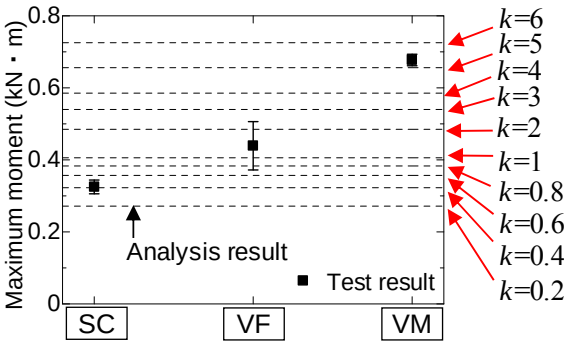

Fig. 13 Maximum bending moment by section analysis and bending test results.

test is shown in Fig. 13. The dotted lines indicate the maximum bending moment calculated by section analysis using each orientation intensity k from 0.2 to 6. The average maximum bending moments in the bending test are plotted by squares with error bars (standard deviation). As shown in Fig. 13, the analysis results in the case of k = 0.4, k = 1, and k = 5 show good agreements with the test results of the SC specimens, VF specimens, and VM specimens, respectively. The difference of bending strength due to the fiber orientation is expressed by the section analysis using the bridging law considering fiber orientation.

6. Conclusions

The authors have proposed the method of calculation of bridging law, which is expressed by tensile stress–crack width relationship, considering the influence of fiber orientation. The calculated bridging law is strongly affected by fiber orientation, which is featured by orientation intensity k. A tri-linear model is newly proposed to express the tensile stress–crack width relationship considering the fiber orientation. Through the bending test, in which the specimens were fabricated by three casting methods to vary the fiber orientation, the followings are found out:

(1) The parameters that give the characteristic points of the tri-linear model are proposed as functions of orientation intensity k.

(2) The maximum loads of the VM specimens (a compacting vibrator is reciprocated longitudinally after FRCC pouring) are twice larger than those obtained by SC specimens.

(3) The results of section analysis, which is conducted to verify the adaptability of the proposed model, can present the difference of bending strength due to the fiber orientation.

Acknowledgments

This study was supported by the JSPS KAKENHI Grant Number 26289188.

References

[1] Rokugo, K., and Kanda, T., Co-Editors. 2013. *Strain Hardening Cement Composites: Structural Design and Performance*. State-of-the-Art Report of the RILEM Technical Committee 208-HFC, SC3, Springer.

[2] Kanakubo, T. 2006. “Tensile Characteristics Evaluation Method for Ductile Fiber-Reinforced Cementitious Composites.” *JCI Journal of Advanced Concrete Technology* 4 (1): 3-17.

[3] Kanakubo, T., Miyaguchi, M., and Asano, K. 2016. “Influence of Fiber Orientation on Bridging Performance of Polyvinyl Alcohol Fiber-Reinforced Cementitious Composite.” *ACI Materials Journal* 113 (2): 131-41.

[4] Li, V. C., Wang, Y., and Backer, S. 1990. “Effect of Inclining Angle, Bundling, and Surface Treatment on Synthetic Fibre Pull-Out from a Cement Matrix.” *Composites* 21 (2): 132-40.

[5] Kanda, T., and Li, V. C. 1998. “Interface Property and Apparent Strength of a High Strength Hydrophilic Fiber in Cement Matrix.” *ASCE Journal of Materials in Civil Engineering* 10 (1): 5-13.

[6] International Organization for Standardization, ISO 19044: 2016. *Test Methods for Fibre-Reinforced Cementitious Composites—Load-Displacement Curve Using Notched Specimen*. Standard by International Organization for Standardization, 11/01/2016.

[7] Laranjeira, F., Aguado, A., Molins, C., Grünewald, S., Walraven, J., and Cavalaro, S. 2012. “Framework to Predict the Orientation of Fibers in FRC: A Novel Philosophy.” *Cement and Concrete Research* 42: 752-68.

[8] Watanabe, K., Ozu, Y., Miyaguchi, M., and Kanakubo, T. 2016. “Influence of Placing Method Considering Fiber Orientation to Bending Characteristics of DFRCC.” *The 7th International Conference of Asian Concrete Federation*, Vol. 1., Paper No.43.